Results in Physics 8 (2018) 552–558

Contents lists available at ScienceDirect

Results in Physics

journal homepage: www.journals.elsevier.com/results-in-physics

On new scaling group of transformation for Prandtl-Eyring fluid model with both heat and mass transfer

Khalil Ur Rehman [a,*], Aneeqa Ashfaq Malik [a], M.Y. Malik [a], M. Tahir [b], Iffat Zehra [c]

[a] Department of Mathematics, Quaid-i-Azam University, Islamabad 44000, Pakistan
[b] Department of Mathematics, Faculty of Basic Sciences, HITEC University, Taxila, Pakistan
[c] Department of Mathematics, Air University, PAF Complex E-9, Islamabad 44000, Pakistan

ARTICLE INFO

Article history:
Received 1 December 2017
Received in revised form 23 December 2017
Accepted 25 December 2017
Available online 29 December 2017

Keywords:
Heat and mass transfer
Scaling group of transformations
Prandtl-Eyring fluid

ABSTRACT

A short communication is structured to offer a set of scaling group of transformation for Prandtl-Eyring fluid flow yields by stretching flat porous surface. The fluid flow regime is carried with both heat and mass transfer characteristics. To seek solution of flow problem a set of scaling group of transformation is proposed by adopting Lie approach. These transformations are used to step down the partial differential equations into ordinary differential equations. The reduced system is solved by numerical method termed as shooting method. A self-coded algorithm is executed in this regard. The obtain results are elaborated by means of figures and tables.

Introduction

The non-Newtonian fluids have non-linear relation between shear stress and shear rate. Some examples of such fluids are ketchup, greases, yogurt, mud, shampoo etc. The study of non-Newtonian fluids is topic of great interest for the past few years. One can see Refs. [1–6] are the few trustful attempts carried out in this regard. Moreover, analysis of distinct non-Newtonian flow models by entertaining various stretching surfaces manifested with pertinent physical effects can be assessed in Refs. [7–21]. In short, owing the important of flow regime aspects of non-Newtonian fluids various fluid models are proposed, namely Maxwell fluid model, Williamson fluid model, Eyring fluid model, Cross fluid model, Ellis fluid model, Casson fluid model, Prandtl, Prandtl-Eyring and Powell-Eyring fluid models are to mention just a few. In 2014, Akbar et al. [22] discussed the dual solution of stagnation point Prantl fluid with magnetic field effects. The solution is obtained by way of shooting method. They found that the velocity is decreases function of both Prantl and elastic parameters. Recently, Khan et al. [23] studied the homogenous-heterogeneous reactions effects on Prandtl fluid flow towards stretching flat surface. They found that in the presence of homogenous-heterogeneous reactions the velocity of Prandtl fluid increases for positive values of Prantl fluid parameters. Further, Kumar et al. [24] discussed the three dimensional Prantl fluid flow towards flat surface. They conclude that in three dimensional frame the velocity profile shows decline nature towards elastic parameter while opposite trend is noticed for Prantl fluid parameter. The physical aspects of nanosized suspended particles in Prantl fluid were investigated by Bilal et al. [25]. They found that the velocity distributions reflects inciting nature for higher values of Prantl parameter. Researchers are still engaged to explore the Prantl and Prantl-Eyring liquids characteristics by considering various physical effects. The recent developments in this direction can be assessed in Ref. [26,27].

In order to solve differential equations, various methods have been used according to nature of differential equation. Sophus Lie discovered Lie group analysis to find the solution of differential equations. This method was consequent from "invariance of differential equation under continuous group of symmetries". A few applications of lie symmetry group are acknowledged in topology, invariant theory, classical mechanics, relativity, differential geometry and many other. The procedure used in this article is the special type of Lie symmetry analysis i.e. scaling group of transformations in order to find out the similarity transformation to convert PDE's into ODE's like Pakdemirli and Yurusoy [28] found the similarity transformations for particular problem. Lie group analysis for flow problem via semi-infinite vertical plate was carried out by Ibrahim et al. [29]. Recently, a detail work is reported on boundary layer flow through Lie symmetry approach by Rehman et al. [30].

The fluid under consideration is non-Newtonian fluid model that is Prandtl-Eyring fluid model. As yet less attention is paid by

* Corresponding author.
E-mail address: krehman@math.qau.edu.pk (K.U. Rehman).

https://doi.org/10.1016/j.rinp.2017.12.071
2211-3797/

Nomenclature

$(\bar{u}, \bar{v})$	Velocity components
(u, v)	dimensionless velocity components
ρ	fluid density
α_T	thermal diffusivity
D_M	mass diffusivity
τ	stress tensor
$\tau_{\bar{x}\bar{y}}$	component of stress tensor
a_1, c_1	fluid material parameters
$T_w(\bar{x})$	surface temperature
T_∞	ambient temperature
$C_w(\bar{x})$	surface concentration
C_∞	ambient concentration
U_0, V_0	reference velocities
L	characteristic length
T_0	reference temperature
C_0	reference concentration
A, β	Prandtl-Eyring fluid parameters
Ω	velocities ratio
d^*	non-dimensional constant
Pr	Prandtl number
Sc	Schmidt number
m	temperature power law index
n	concentration power law index
p, q, r, s, t, t_1, t_2	constants
$\bar{\omega}$	Lie group parameter
B	integral constant
ψ	stream function
$f'(\xi)$	Prandtl-Eyring fluid velocity
$\theta(\xi)$	Prandtl-Eyring fluid temperature
$\phi(\xi)$	Prandtl-Eyring fluid concentration
f_q	suction/injection parameter
$\sqrt{\mathrm{Re}_x}\, C_f$	skin friction coefficient
$\frac{Nu}{\sqrt{\mathrm{Re}_x}}$	Nusselt number
$\frac{Sh}{\sqrt{\mathrm{Re}_x}},$	Sherwood number
Re_x	Reynolds number
$q_1, q_2, q_3, q_4, q_5, q_6, q_7$	dummy variables
$\alpha_1, \alpha_2, \alpha_3$	initial guess values
U_∞	ambient velocity
u_e	free stream velocity
u_w	stretching velocity

researchers to inspect the flow field characteristics of Prandtl-Eyring fluid. The reason behind is the arising of non-linear flow narrating differential equations. The solution of these equations is one of the difficult task due to complex structured. In this attempt we have proposed a set of similarity transformation by way of Lie approach. These transformations are very helpful to seek out the solution of differential system yielded through Prandtl-Eyring fluid model especially when both the thermal and concentration individualities are taken into account.

Mathematical modelling

Consider a steady incompressible non-Newtonian Prandtl-Eyring fluid flow over a two-dimensional semi-infinite stretched plate having velocity $u_w(\bar{x})$. The plate is assumed to be porous with the velocity $v_w(\bar{x})$ along $\bar{y}-axis$, (See Fig. 1). The reduced continuity, momentum, energy and concentration equations under boundary layer approximation are

$$\frac{\partial \bar{u}}{\partial \bar{x}} + \frac{\partial \bar{v}}{\partial \bar{y}} = 0, \tag{1}$$

$$\bar{u}\frac{\partial \bar{u}}{\partial \bar{x}} + \bar{v}\frac{\partial \bar{u}}{\partial \bar{y}} = \frac{1}{\rho}\frac{\partial \tau_{\bar{x}\bar{y}}}{\partial \bar{y}}, \tag{2}$$

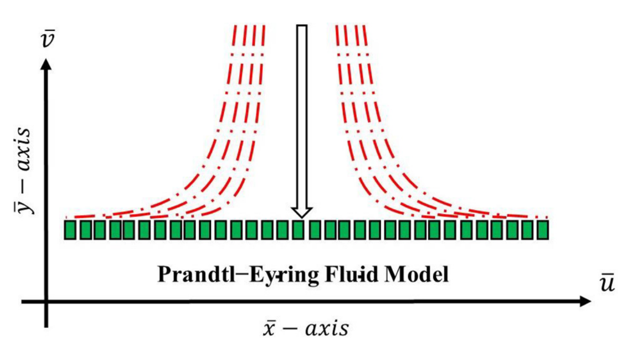

Fig. 1. Geometry of flow problem.

$$\bar{u}\frac{\partial \bar{T}}{\partial \bar{x}} + \bar{v}\frac{\partial \bar{T}}{\partial \bar{y}} = \alpha_T\frac{\partial^2 \bar{T}}{\partial \bar{y}^2}, \tag{3}$$

$$\bar{u}\frac{\partial \bar{C}}{\partial \bar{x}} + \bar{v}\frac{\partial \bar{C}}{\partial \bar{y}} = D_M\frac{\partial^2 \bar{C}}{\partial \bar{y}^2}, \tag{4}$$

where, $\bar{u}, \bar{v}$ are the velocity components taken along $\bar{x}, \bar{y}$ direction respectively, τ, ρ, α_T and D_M denotes shear stress, fluid density, thermal diffusivity and mass diffusivity respectively. For Prandtl-Eyring fluid the stress tensor is given by form

$$\tau = \left[\frac{a_1 \operatorname{arc\,sinh}\left(\frac{1}{c_1}\sqrt{\frac{1}{2}\mathrm{trace}\,(\mathrm{A}_1^2)}\right)}{\sqrt{\frac{1}{2}\mathrm{trace}\,(\mathrm{A}_1^2)}}\right]\mathrm{A}_1, \tag{5}$$

here, a_1 and c_1 refers to material parameters of fluid and A_1 is first Rivilin-Erickson tensor.

The required component of Prandtl-Eyring fluid is given by

$$\tau_{\bar{x}\bar{y}} = \left[\frac{a_1}{\rho}\operatorname{arc\,sinh}\left(\frac{1}{c_1}\frac{d\bar{u}}{d\bar{y}}\right)\right],$$

through the Taylor series expansion of $\sinh^{-1}\left(\frac{1}{c_1}\left(\frac{\partial \bar{u}}{\partial \bar{y}}\right)\right)$, we consider first two terms and neglect higher order i.e. $\sinh^{-1}\left(\frac{1}{c_1}\left(\frac{\partial \bar{u}}{\partial \bar{y}}\right)\right) = \frac{1}{c_1}\left(\frac{\partial \bar{u}}{\partial \bar{y}}\right) - \frac{1}{6}\left(\frac{1}{c_1}\frac{\partial \bar{u}}{\partial \bar{y}}\right)^3$. Substituting the value in Eq. (2) along with stagnation point assumption we arrive at

$$\bar{u}\frac{\partial \bar{u}}{\partial \bar{x}} + \bar{v}\frac{\partial \bar{u}}{\partial \bar{y}} = u_e\frac{\partial u_e}{\partial x} + \frac{a}{\rho c_1}\left(\frac{\partial^2 \bar{u}}{\partial \bar{y}^2}\right) - \frac{a}{2\rho c_1^3}\left(\frac{\partial \bar{u}}{\partial \bar{y}}\right)^2\left(\frac{\partial^2 \bar{u}}{\partial \bar{y}^2}\right), \tag{6}$$

the boundary conditions of problem are

$$\bar{u} = U_0 u_w(\frac{\bar{x}}{L}), \bar{T} - T_\infty = T_0 T_w(\frac{\bar{x}}{L}), \bar{v} = V_0 v_w\left(\frac{\bar{x}}{L}\right),$$

$$\bar{C} - C_\infty = C_0 C_w\left(\frac{\bar{x}}{L}\right), \text{ at } \bar{y} = 0, \tag{7}$$

$$\bar{u} \to U_\infty u_e\left(\frac{\bar{x}}{L}\right), \bar{T} \to T_\infty, \bar{C} \to C_\infty, \text{at } \bar{y} \to \infty,$$

where, $T_w(\bar{x})$ and T_∞ stands for the surface temperature and ambient temperature, whereas $C_w(\bar{x})$ and C_∞ stands for the surface concentration and ambient concentration respectively while U_0, V_0, U_∞ and L stands for reference velocities, ambient velocity and characteristics length, T_0 and C_0 denotes reference temperature and reference concentration respectively. Introducing the following non-dimensional parameters

$$u=\frac{\bar{u}}{U_\infty},\ x=\frac{\bar{x}}{L},\ v=\frac{\bar{v}}{U_\infty}\left(\frac{U_\infty L}{\nu}\right)^{\frac{1}{2}}, y=\frac{\bar{y}}{L}\left(\frac{U_\infty L}{\nu}\right)^{\frac{1}{2}},\quad T=\frac{\bar{T}-T_\infty}{T_0},\ C=\frac{\bar{C}-C_\infty}{C_0}, \tag{8}$$

by incorporating these one can obtain

$$\frac{\partial u}{\partial x}+\frac{\partial v}{\partial y}=0, \tag{9}$$

$$u\frac{\partial u}{\partial x}+v\frac{\partial u}{\partial y}=u_e\frac{\partial u_e}{\partial x}+A\frac{\partial^2 u}{\partial y^2}-A\beta\left(\frac{\partial u}{\partial y}\right)^2\frac{\partial^2 u}{\partial y^2}, \tag{10}$$

$$u\frac{\partial T}{\partial x}+v\frac{\partial T}{\partial y}=\frac{1}{\Pr}\frac{\partial^2 T}{\partial y^2}, \tag{11}$$

$$u\frac{\partial C}{\partial x}+v\frac{\partial C}{\partial y}=\frac{1}{Sc}\frac{\partial^2 C}{\partial y^2}, \tag{12}$$

with reduced conditions

$$u=U=\Omega u_w(x),\ T=T_w(x),\ v=d^\bullet v_w(x),\ C=C_w(x),\ \text{when } y=0,\quad u=u_e,\ T=0,\ C=0,\ \text{when } y\to\infty, \tag{13}$$

where A, β denotes fluid parameters and Ω, $d^\bullet$ denotes velocities ratio, non-dimensional constant while Pr and Sc refers to Prandtl number and Schmidt number respectively. These quantities are defined as

$$A=\frac{a_1}{\mu c_1},\ \beta=\frac{U_\infty^3}{2c_1^2\nu L},\ \Pr=\frac{\nu}{\alpha_T},\ Sc=\frac{\nu}{D},\ d^\bullet=\frac{V_0}{U_\infty}\left(\frac{U_\infty L}{\nu}\right)^{\frac{1}{2}}, \tag{14}$$

the forms for velocities, surface temperature and concentration are considered as

$$u_w(x)=x^{\frac{1}{3}},\ v_w(x)=x^{-\frac{1}{3}},\ T_w(x)=x^m,\ C_w(x)=x^n, \tag{15}$$

where m, n shows temperature and concentration power index accordingly.

Scaling transformations

Now the system of Lie group of transformation is entertain to attain the similarity transformations that is

$$\Lambda:\ x^*=xe^{\bar{\omega}p},\ y^*=ye^{\bar{\omega}q},\ u^*=ue^{\bar{\omega}r},\ v^*=ve^{\bar{\omega}s},\quad T^*=Te^{\bar{\omega}t},\ C^*=Ce^{\bar{\omega}t_1},\ u_e^*=u_e e^{\bar{\omega}t_2}, \tag{16}$$

where p, q, r, s, t, t_1 and t_2 are constants which are to be determined and $\bar{\omega}$ is Lie group parameter. The Eq. (16) will transforms (x, y, u, v, T, C, u_e) into co-ordinates$(x^*, y^*, u^*, v^*, T^*, C^*, u_e^*)$. By utilizing Eq. (16) on Eqs. (9)–(12), one can obtain

$$\frac{\partial u^*}{\partial x^*}+e^{\bar{\omega}(-p+q+r-s)}\frac{\partial v^*}{\partial y^*}=0, \tag{17}$$

$$u^*\frac{\partial u^*}{\partial x^*}+e^{\bar{\omega}(-p+q+r-s)}v^*\frac{\partial u^*}{\partial y^*}=e^{\bar{\omega}(2r-2u)}u_e^*\frac{\partial u_e^*}{\partial x^*}+Ae^{\bar{\omega}(-p+2q+r)}\frac{\partial^2 u^*}{\partial y^{*2}}-A\beta e^{\bar{\omega}(-p+4q-r)}\frac{\partial^2 u^*}{\partial y^{*2}}\left(\frac{\partial u^*}{\partial y^*}\right)^2, \tag{18}$$

$$u^*\frac{\partial T^*}{\partial x^*}+e^{\bar{\omega}(-p+q+r-s)}v^*\frac{\partial T^*}{\partial y^*}=\frac{1}{Pr}e^{\bar{\omega}(-p+2q+r)}\frac{\partial^2 T^*}{\partial y^{*2}}, \tag{19}$$

$$u^*\frac{\partial C^*}{\partial x^*}+e^{\bar{\omega}(-p+q+r-s)}v^*\frac{\partial C^*}{\partial y^*}=\frac{1}{Sc}e^{\bar{\omega}(-p+2q+r)}\frac{\partial^2 C^*}{\partial y^{*2}}, \tag{20}$$

$$u^*(x^*,0)=\Omega e^{\bar{\omega}(r-1/3)}x^{1/3^*},T^*=e^{\bar{\omega}(t-m)}x^{m^*},\ v^*(x^*,0)=d^\bullet e^{\bar{\omega}(s+1/3)}x^{-1/3^*},\quad C^*=e^{\bar{\omega}(t_1-n)}x^{n^*},\ u^*(x^*,\infty)=u_e^*e^{\bar{\omega}(r-t_2)},\ T^*(x^*,\infty)=0,\ C^*(x^*,\infty)=0, \tag{21}$$

with the concern of the group transformationsΛ, an invariance of Eqs. (17)–(21) is attained and Eq. (15) must satisfy the following relations

$$-p+q+r-s=0,\ r-u=0,\quad -p+2q+r=0,\ -p+4q-r=0, \tag{22}$$

evaluating these equation in term of parameter p, we get

$$q=r=t_2=\frac{p}{3},\ s=\frac{-p}{3},\ t=m,\ t_1=n, \tag{23}$$

the scaling transformation admitted by Eqs. (9)–(12) reduces to following form

$$\Lambda:\ x^*=xe^{\bar{\omega}p},\ y^*=y^{\bar{\omega}p/3},\ u^*=ue^{\bar{\omega}p/3},\ v^*=ve^{-\bar{\omega}p/3},\quad T^*=Te^{\bar{\omega}m},\ C^*=Ce^{\bar{\omega}n},\ u_e^*=u_e e^{\bar{\omega}p/3}, \tag{24}$$

now expanding through Taylor series the exponentials in Eq. (24) up-to order $\bar{\omega}$,we acquire

$$\Lambda:\begin{cases} x^*-x=\bar{\omega}px, y^*-y=\frac{\bar{\omega}p}{3}y, u_e^*-u_e=\frac{\bar{\omega}p}{3}u_e, T^*-T=\bar{\omega}mT,\\ u^*-u=\frac{\bar{\omega}p}{3}u,\ v^*-v=-\frac{\bar{\omega}p}{3}v, C^*-C=\bar{\omega}nC,\end{cases} \tag{25}$$

the characteristic equation as succeeding denotes the differences between transformed and original variables as a differentials and equating each term one can obtain

$$\frac{dx}{px}=\frac{dy}{\frac{p}{3}y}=\frac{du}{\frac{p}{3}u}=\frac{dv}{-\frac{p}{3}v}=\frac{du_e}{\frac{p}{3}u_e}=\frac{dT}{mT}=\frac{dC}{nC}. \tag{26}$$

Assuming $p=1$ and solving the equations stated above we obtain

$$\xi=yx^{-1/3},\ u=x^{1/3}\frac{df(\xi)}{d\xi},\ v=x^{-1/3}h(\xi),\quad T=x^m\theta(\xi),\ C=x^n\phi(\xi),\ u_e=Bx^{1/3}, \tag{27}$$

where B is the integral constant and taken to be unity. Therefore through the scaling transformation, the free stream velocity is found to be $x^{1/3}$ which give emphasis to define free stream $u_e(x)$ in terms of surface stretching velocity. Now, $h(\xi)$ is to be evaluated by continuity equation. The stream function (ψ) in terms of velocity components cab be written as

$$u=\frac{\partial\psi}{\partial y}, v=-\frac{\partial\psi}{\partial x}, \tag{28}$$

Eqs. (27) and (28) gives

$$\psi=x^{2/3}h(\xi), \tag{29}$$

then $h(\xi)$ will become

$$h(\xi)=\frac{-1}{3}\left(2f(\xi)-\xi\frac{df(\xi)}{d\xi}\right), \tag{30}$$

using Eq. (27) along with Eq. (30), one can reduced the Eqs. (9)–(13) into

$$A\frac{d^3f(\xi)}{d\xi^3}-A\beta\left(\frac{d^2f(\xi)}{d\xi^2}\right)^2\frac{d^3f(\xi)}{d\xi^3}+\frac{2}{3}f(\xi)\frac{d^2f(\xi)}{d\xi^2}-\frac{1}{3}\left(\frac{df(\xi)}{d\xi}\right)^2+\frac{1}{3}=0, \tag{31}$$

$$\frac{d^2\theta(\xi)}{d\xi^2}+\Pr\left(\frac{2}{3}f(\xi)\frac{d\theta(\xi)}{d\xi}-m\frac{df(\xi)}{d\xi}\theta(\xi)\right)=0, \tag{32}$$

$$\frac{d^2\phi(\xi)}{d\xi^2}+Sc\left(\frac{2}{3}f(\xi)\frac{d\phi(\xi)}{d\xi}-n\frac{df(\xi)}{d\xi}\phi(\xi)\right)=0, \tag{33}$$

with

$$\begin{aligned}&\frac{df(\xi)}{d\xi}=\Omega,\ f(\xi)=f_q,\ \theta(\xi)=1,\ \phi(\xi)=1,\ \text{at}\ \xi=0,\\&\frac{df(\xi)}{d\xi}\to 1,\ \theta(\xi)\to 0,\ \phi(\xi)\to 0,\ \text{when}\ \xi\to\infty,\end{aligned} \tag{34}$$

where m and n are temperature power law index and concentration power law index respectively. In addition, $f_q=-\frac{3}{2}d^{\bullet}$ is non-dimensional parameter constant, $f_q<0$ relates to injection and $f_q>0$ relates to suction. The skin friction coefficient, Nusselt number and Sherwood number are the required physical quantities of the problem which are defined as

$$\begin{aligned}&C_f=\frac{\tau_w}{\rho U^2},\ Nu=\frac{xq_w}{\alpha_T(T_w(x)-T_\infty)},\ Sh=\frac{xj_w}{D_M(C_w(x)-C_\infty)},\\&\tau_w=\left[\frac{a_1}{c_1}\frac{\partial u}{\partial y}-\frac{a_1}{6c_1^3}\left(\frac{\partial u}{\partial y}\right)^3\right]_{y=0},\ q_w=-\alpha_T\left(\frac{\partial T}{\partial y}\right)_{y=0},\ j_w=-D_M\left(\frac{\partial C}{\partial y}\right)_{y=0},\end{aligned} \tag{35}$$

the reduced forms are

$$\begin{aligned}&\sqrt{\mathrm{Re}_x}C_f=Af''(0)-A\beta[f''(0)]^3,\ \frac{Nu}{\sqrt{\mathrm{Re}_x}}=-\theta'(0),\\&\frac{Sh}{\sqrt{\mathrm{Re}_x}}=-\phi'(0)\ \text{where}\ \mathrm{Re}_x=\frac{U_0x}{\nu L}.\end{aligned} \tag{36}$$

Numerical formulation

To implement shooting method let us introduce dummy variables for order reduction. The fresh variables are allocated as

$$\begin{aligned}q_1&=f(\xi),\\q_2&=\frac{df(\xi)}{d\xi},\\q_3&=\frac{df^2(\xi)}{d\xi^2},\\q_4&=\theta(\xi),\\q_5&=\frac{d\theta(\xi)}{d\xi},\\q_6&=\phi(\xi),\\q_7&=\frac{d\phi(\xi)}{d\xi},\end{aligned} \tag{37}$$

by incorporating these relations, the Eqs. (30)–(33) takes the form

$$\begin{aligned}q_1'&=q_2,\\q_2'&=q_3,\\q_3'&=\frac{(q_2^2-2q_1q_3-1)}{3(A-A\beta q_3^2)},\\q_4'&=q_5,\\q_5'&=\frac{\Pr(3mq_2q_4-2q_1q_5)}{3},\\q_6'&=q_7,\\q_7'&=\frac{Sc(3nq_2q_6-2q_1q_7)}{3},\end{aligned} \tag{38}$$

the end point conditions in terms of new variable are

$$\begin{aligned}q_1(0)&=f_q,\\q_2(0)&=\Omega,\\q_3(0)&=\alpha_1,\\q_4(0)&=1,\\q_5(0)&=\alpha_2,\\q_6(0)&=1,\\q_7(0)&=\alpha_3,\end{aligned} \tag{39}$$

where α_1,α_2 and α_3 are the initial guesses

The extreme conditions are

$$q_2(\xi)\to 1,\ q_4(\xi)\to 0,\ q_6(\xi)\to 0,\ \text{as}\ \xi\to\infty. \tag{40}$$

Results and discussion

The Prandtl-Eyring fluid flow over a porous stretching sheet in a parallel free stream is considered. The obtained results are offered by both graphs and tables. Particularly, Table 1–3 shown the impact of physical parameters on skin friction coefficient, Nusselt number, and Sherwood number. Explicitly Table 1 shows the impact of fluid parameters and suction/injection parameter on skin friction coefficient. It is observed that the skin friction is increasing function of fluid parameter A whereas it is decreasing function for fluid parameter β. For suction/injection parameter, the skin friction is an increasing function. The skin friction coefficient values implies the amount of drag force exerted on Prandtl-Eyring fluid particles in flow regime. Table 2 displays the nature of Prandtl number, temperature power index and suction /injection parameter and it is notified that the Nusselt number reflects inciting values for positive values of Prandtl number and suction/injection parameter but it turns to be a constant for temperature power index. The influence of Schmidt number, concentration power index and suction/injection parameter is elaborated through Table 3. It is observed that the Sherwood number is an increasing function of all parameters as mention in Table 3. The numerical values of both Nusselt and Sherwood numbers highlighted the magnitude of transfer of heat and mass respectively normal to the flat surface. Figs. 2–7 are design to inspect the impact of fluid parameters, Prandtl number, temperature power law index, Schmidt number, and concentration power law index on dimensionless velocity, temperature and concentration. To be more specific, the impact of fluid parameters A and β are examined and offered through Figs. 2 and 3 respectively. It is observed that the fluid velocity shows inciting curves for positive values of fluid parameter A but an opposite trend is noticed for large value of fluid parameter β, see Fig. 3. The variations in temperature are tested for higher values of Prandtl number and temperature power law index. Figs. 4 and 5 are constructed in this regard. It is seen that the fluid temperature is decreasing function of Prandtl number. The Prandtl number admits inverse relation with thermal diffusivity. Therefore, flow regime with higher values of Prandtl number is the source of drop of fluid temperature. Similar trend is observed for higher values of temperature power law index towards fluid temperature, see Fig. 5. The variations in concentration distribution are examined for both Schmidt number and concentration power law index. Figs. 6 and 7 enclosed the obtain observations in this regard. Fig. 6 is the evident that the concentration profile is decreasing function of higher values of Schmidt number. This effect is quite similar with the variations of temperature against Prandtl number. Here, the rate of mass diffusivity is inversely proportional to large values of Schmidt number. Fig. 7 reports the concentration curves for higher values of concentration power law

Table 1
Distinction in SFC values for A, β and f_q.

A	β	f_q	$f''(0)$	$C_f\sqrt{Re_x} = Af''(0) - A\beta[f''(0)]^3$
0.2	0.1	0.1	1.1458	0.1991
0.3	0.1	0.1	0.9076	0.2498
0.4	0.1	0.1	0.7734	0.2908
0.1	−0.3	0.1	1.4194	0.2277
0.1	−0.2	0.1	1.4705	0.2106
0.1	−0.1	0.1	1.5358	0.1898
0.1	0.1	−0.3	0.9401	0.0857
0.1	0.1	−0.2	1.0994	0.0966
0.1	0.1	−0.1	1.2875	0.1074

Table 2
Distinction in Nusselt number for $\Pr, m$ and f_q.

Pr	m	f_q	$\frac{Nu}{\sqrt{Re_x}} = -\theta'(0)$
1.1	0.1	0.1	1.0613
1.2	0.1	0.1	1.1065
1.3	0.1	0.1	1.1498
0.1	0.2	0.1	0.9642
0.1	0.3	0.1	0.9642
0.1	0.4	0.1	0.9642
0.1	0.1	0.2	0.3500
0.1	0.1	0.3	0.3543
0.1	0.1	0.4	0.3586

Table 3
Distinction in Sherwood number for Sc, n and f_q.

Sc	n	f_q	$\frac{Sh}{\sqrt{Re_x}} = -\phi'(0)$
0.7	0.1	0.1	0.5516
0.8	0.1	0.1	0.5891
0.9	0.1	0.1	0.6245
0.6	0.2	0.1	0.6711
0.6	0.3	0.1	0.7147
0.6	0.4	0.1	0.7558
0.6	0.1	0.2	0.6615
0.6	0.1	0.3	0.6993
0.6	0.1	0.4	0.7377

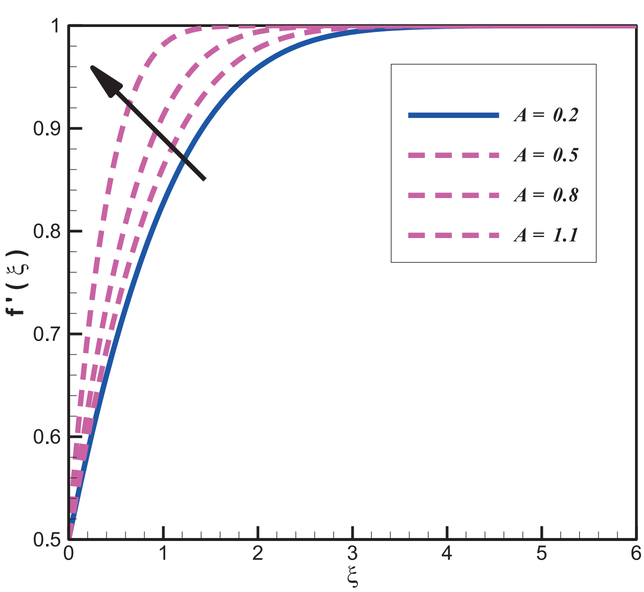

Fig.2. Influence of fluid parameter A on velocity profile.

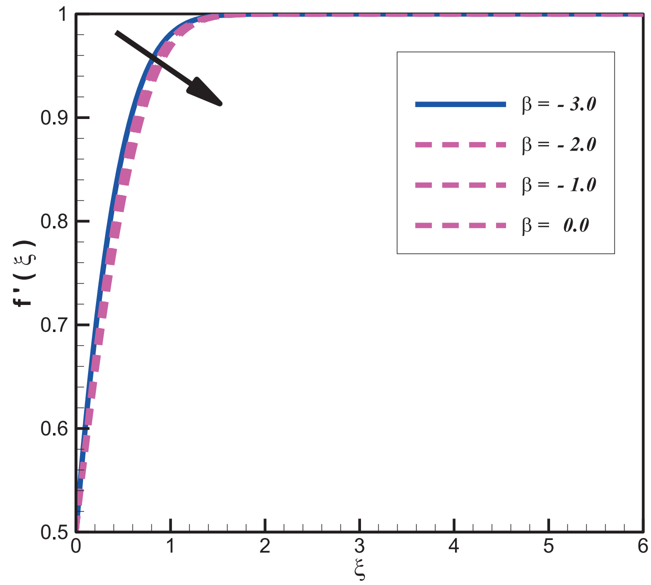

Fig.3. Influence of fluid parameter β on velocity profile.

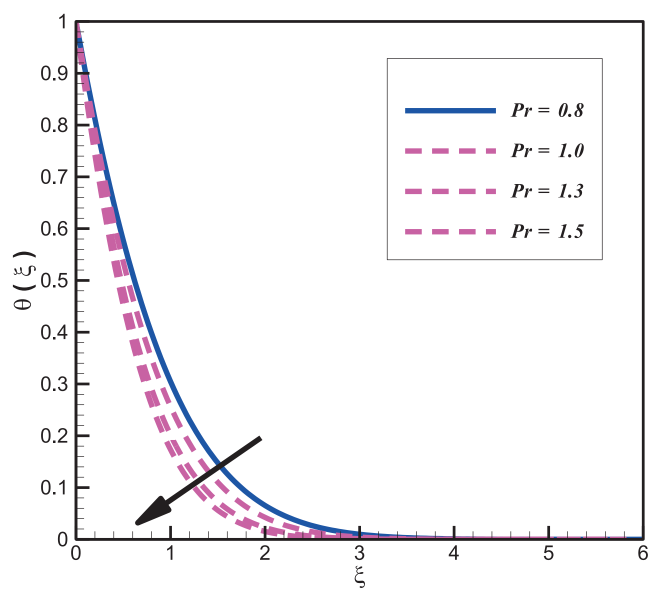

Fig. 4. Influence of Prandtl number Pr on temperature profile.

index. It is observed that the concentration profile is diminishing function of concentration power law index.

Closing remarks

The prime objective of present attempt is to provide the scaling group of transformation for Prandtl-Eyring fluid model by way of Lie group approach especially when thermal and concentration individualities are considered at a time. A numerical solution is

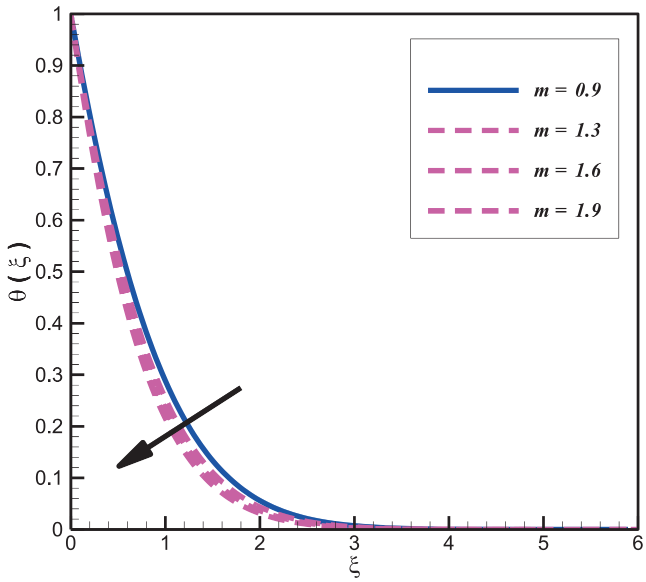

Fig. 5. Influence of temperature power index m on temperature profile.

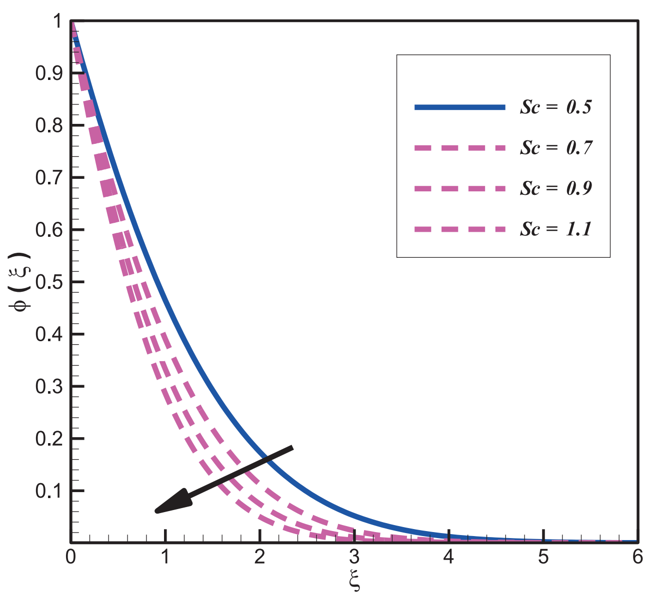

Fig. 6. Influence of Schmidt number Sc on concentration profile.

provided by self-coded computational algorithm. The key observations are itemized as follows

1. Set of scaling group of transformation is proposed for Prandtl-Eyring fluid when both temperature and concentration effects are taken into account.
2. The Prandtl-Eyring fluid velocity is decreasing function of fluid parameters β, but opposite trend is noticed via fluid parameter A.
3. Temperature shows decline curves for both Prandtl and temperature power law index.
4. Concentration is diminishing function of both Schmidt number and concentration power law index
5. The SFC is an increasing function of suction/injection parameter and fluid parameter A but it shows opposite trend for fluid parameter β.

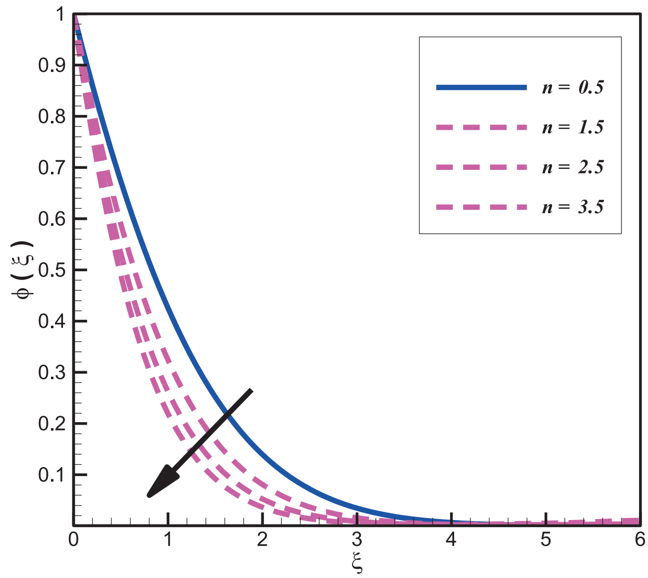

Fig. 7. Influence of concentration power index n on concentration profile.

6. Nusselt number shows inciting values for both Prandtl number and suction/injection parameter while it shows constant nature for the temperature power law index.
7. Sherwood number surprisingly found to be increasing function of Schmidt number, concentration power index and suction/injection parameter.

References

[1] Tripathi S, Bhattacharya A, Singh R, Tabor RF. Lubricated transport of highly viscous non-newtonian fluid as core-annular flow: a CFD study. Procedia IUTAM 2015;15:278–85.

[2] Rahimi-Gorji M, Pourmehran O, Gorji-Bandpy M, Ganji DD. An analytical investigation on unsteady motion of vertically falling spherical particles in non-Newtonian fluid by collocation method. Ain Shams Eng. J. 2015;6(2):531–40.

[3] Ciriello V, Longo S, Chiapponi L, Di Federico V. Porous gravity currents of non-Newtonian fluids within confining boundaries. Proc. Environ. Sci. 2015;25:58–65.

[4] Aldi N, Buratto C, Pinelli M, Spina PR, Suman A, Casari N. CFD analysis of a non-newtonian fluids processing pump. Energy Procedia 2016;101:742–9.

[5] Moosavi M, Momeni M, Tavangar T, Mohammadyari R, Rahimi-Esbo M. Variational iteration method for flow of non-Newtonian fluid on a moving belt and in a collector. Alexandria Eng. J. 2016;55(2):1775–83.

[6] Feng S, Chen Q. Analysis on non-newtonian characteristics for nano magnetic fluid. Procedia Eng. 2017;174:1208–14.

[7] Bachok N, Ishak A, Pop I. Unsteady boundary-layer flow and heat transfer of a nanofluid over a permeable stretching/shrinking sheet. Int. J. Heat Mass Transfer 2012;55(7):2102–9.

[8] Sreelakshmi K, Nagendramma V. Study of thermophoresis on the MHD flow due to an exponentially stretching sheet in the presence of viscous dissipation. Proc. Eng. 2015;127:340–6.

[9] Das K. Nanofluid flow over a non-linear permeable stretching sheet with partial slip. J. Egypt. Math. Soc. 2015;23(2):451–6.

[10] Hayat T, Bashir G, Waqas M, Alsaedi A. MHD flow of Jeffrey liquid due to a nonlinear radially stretched sheet in presence of Newtonian heating. Results Phys. 2016;6:817–23.

[11] Eid MR. Chemical reaction effect on MHD boundary-layer flow of two-phase nanofluid model over an exponentially stretching sheet with a heat generation. J. Mol. Liq. 2016;220:718–25.

[12] Kumar KG, Gireesha BJ, Rudraswamy NG, Manjunatha S. Radiative heat transfers of Carreau fluid flow over a stretching sheet with fluid particle suspension and temperature jump. Results Phys. 2017.

[13] Rehman KU, Qaiser A, Malik MY, Ali U. Numerical communication for MHD thermally stratified dual convection flow of Casson fluid yields by stretching cylinder. Chin. J. Phys. 2017.

[14] Malik MY, Bilal S, Bibi M. Numerical analysis for MHD thermal and solutal stratified stagnation point flow of Powell-Eyring fluid induced by cylindrical surface with dual convection and heat generation effects. Results Phys. 2017;7:482–92.

[15] Seth GS, Mishra MK. Analysis of transient flow of MHD nanofluid past a non-linear stretching sheet considering Navier's slip boundary condition. Adv. Powder Technol. 2017;2(28):375–84.

[16] Bilal S, Rehman KU, Malik MY. Numerical investigation of thermally stratified Williamson fluid flow over a cylindrical surface via Keller box method. Results Phys. 2017;7:690–6.
[17] Rehman KU, Malik AA, Malik MY, Sandeep N, Saba NU. Numerical study of double stratification in Casson fluid flow in the presence of mixed convection and chemical reaction. Results Phys. 2017;7:2997–3006.
[18] Malik MY, Bilal S, Bibi M, Ali U. Logarithmic and parabolic curve fitting analysis of dual stratified stagnation point MHD mixed convection flow of Eyring-Powell fluid induced by an inclined cylindrical stretching surface. Results Phys. 2017;7:544–52.
[19] Rehman KU, Malik MY, Makinde OD, Malik AA. A comparative study of nanofluids flow yields by an inclined cylindrical surface in a double stratified medium. Eur. Phys. J. Plus 2017;132(10):427.
[20] Rehman KU, Khan AA, Malik MY, Zehra I, Ali U. Temperature and concentration stratification effects on non-Newtonian fluid flow past a cylindrical surface. Results Phys. 2017;7:3659–67.
[21] Rehman KU, Khan AA, Malik MY, Pradhan RK. Combined effects of Joule heating and chemical reaction on non-Newtonian fluid in double stratified medium: a numerical study. Results Phys. 2017;7:3487–96.
[22] Akbar NS, Khan ZH, Haq RU, Nadeem S. Dual solutions in MHD stagnation-point flow of Prandtl fluid impinging on shrinking sheet. Appl. Math. Mech. 2014;35(7):813–20.
[23] Khan I, Malik MY, Hussain A, Salahuddin T. Effect of homogenous-heterogeneous reactions on MHD Prandtl fluid flow over a stretching sheet. Results Phys. 2017;7:4226–31.
[24] Kumar KG, Rudraswamy NG, Gireesha BJ. Effects of mass transfer on MHD three dimensional flow of a Prandtl liquid over a flat plate in the presence of chemical reaction. Results Phys. 2017;7:3465–71.
[25] Bilal S, Rehman KU, Malik MY, Hussain A, Awais M. Effect logs of double diffusion on MHD Prandtl nano fluid adjacent to stretching surface by way of numerical approach. Results Phys. 2017;7:470–9.
[26] Iftikhar N, Rehman A. Peristaltic flow of an Eyring Prandtl fluid in a diverging tube with heat and mass transfer. Int. J. Heat Mass Transfer 2017;111:667–76.
[27] Dominic Breit, Prandtl Eyring fluid in Existence theory for Generalized Newtonian fluids, 2017, pages 89–97.
[28] Pakdemirli M, Yurusoy M. Similarity transformations for partial differential equations. SIAM Rev. 1998;40(1):96–101.
[29] Ibrahim F, Mansour M, Hamad MA. Lie-group analysis of radiative and magnetic field effects on free convection and mass transfer flow past a semi-infinite vertical flat plate. Electron. J. Differ. Equ. (EJDE) [electronic only] 2005. Paper-No.
[30] Rehman KU, Malik AA, Malik MY, Hayat T. Generalized Lie symmetry analysis for non-linear differential equations: a purely viscous fluid model. Results Phys. 2017;7:3537–42.